Thermodynamic model of freeze-drying of poultry breast using infrared thermography

Tomas-Egea, J.A.[a]; Castro-Giraldez, M.[a]; Fito, P.J.[a*]

[a] Instituto Universitario de Ingeniería de Alimentos para el Desarrollo. Universitat Politècnica de València, Valencia, Spain

*pedfisu@tal.upv.es

Abstract

Food dehydration is one of a main process to preserve meal. In order to optimaze a freeze-drying operation a physic model is needed to well describe the thermodynamic behaviors involved in this process. In this work, a thermographic camera and different physico-chemical determinations are used to monitor many phenomena that occur during the lyophilization of poultry breast. Finally, a non-continuous irreversible thermodynamic model, based on thermal infrared measures and in shrinkage/swelling mechanism, has been developed, wich explains the behaviours produced throughout the meat freeze-drying process.

Keywords: freeze-drying, thermodynamic model, infrared thermography, poultry.

1. Introduction

Lyophilization is a drying process that consists in sublimate ice into vapour, producing water desorption, and one possibility can be to bring the product below the triple point (273.16 K and 611.73 Pa) of the water state diagram. This process gets very low water activities and does not heat the product, which is an advantage when thermolabile compounds are present[1,2,3]. Once the product has frozen below its eutectic point and generated vacuum, the product begins the elimination of water in two consecutive phases: sublimation and evaporation. When the frozen product reaches the vapor pressure, the freezing water fraction of the product is sublimated starting from the surface, creating a sublimation front that advances towards the center. With the advance of the front, there is a zone that has sublimated the freezing water, but still has water adsorbed as liquid phase[4,5]. The steam, coming from the front, causes a mechanical drag of the adsorbed water, which removes it and causes its desorption by evaporation.

Considering the importance of dehydration processes to conserve food, it is necessary to study them closely. For this, the process can be modeled with equations such as the Gibbs free energy, which can describe the thermodynamic behavior of the food throughout the process. These equations have been used previously in orange peel[6] and pork meat[7]. The water transport its also modeled in pork meat[8] and tomato[9]. Also, another freeze-dried products has been modeled like Strawberries[10] or black currant juice[11] as well as generic mathematical models[12].

Infrared thermography is a technique that allows to predict the temperature along a surface by receiving the flow of photons emitted by a body. Therefore, the possibility of monitoring the process with this technology gives us the ability to develop kinetic models of drying, thanks to the possibility of follow the temperature distribution over a surface, over a period of time[13].

The aim of this research is the development of a thermodynamic model of freezedrying process of poultry meat using infrared thermography.

2. Materials and Methods

2.1. Experimental procedure

For the experimental phase, poultry breast samples (*Pectoralis major*) were used. Cylinders of 2 cm in diameter and 2 cm in height were obtained by a punch. The cutting of the cylinders was perpendicular to the fibers. Two cylinders were used for each lyophilization and this operation was carried out in triplicate. The samples were frozen at -40 °C and introduced into the dry chamber of the lyophilizer, at a distance of 1.5 cm between them. During the

lyophilization, the temperature of the surface in one of the two chicken cylinders, as well as the reference material and the environment was controlled by type K thermocouples. In addition, the thermographic camera was introduced inside the lyophilizer for a continuous recording of the process.

In order to characterize the samples, this determinations were made before and after the lyophilization: mass, water activity, humidity and volume. In addition, the density of frozen and lyophilized product was determined.

2.2. Physico-chemical measurements

The mass of the samples was determined with a Mettler Toledo AB304-S balance, with an accuracy of $\pm$ 0.001 g. The humidity of the sample was obtained following the ISO 1442 (1997) standard for meat products, drying the samples at 110 ℃ and atmospheric pressure for 48 hours until reach a constant mass. The water activity was determined with a dew point hygrometer Aqualab®, series 3 TE, with an accuracy of $\pm$ 0.003. The volume was determined by image analysis, using Adobe © Photoshop © CS6 software. The density of frozen and lyophilized sample was determined by the pyknometer method. All measurements were made in triplicate.

2.3. Freeze drying operation

The thermographic camera was placed at 15 cm from the samples, with an angle of 0° and focusing the flat surface of the cylindrical samples. A reference material of known emissivity ($\varepsilon = 0.95$) (Optris GmbH, Berlin, Germany) was placed between both samples.

The control of the temperature during the lyophilization, the inside, the reference material and the sample, was carried out with three K-type thermocouples, all of them connected to an Agilent 34901A multiplexer (Agilent Technologies, Malaysia); for the automatic recording of the measurements, the Agilent data acquisition equipment 34972A (Agilent Technologies, Malaysia) was used. The internal pressure control was carried out with the lyophilizer's own pressure sensor.

The lyophilizer used for the experimental was the Lioalfa-6 from Telstar, Germany. With a working pressure of 35 to 50 Pa and a cooling circuit at -45 ℃. All the cables and sensors necessary for the data collection were introduced in the dry chamber replacing the original stopper of the lyophilizer with one of rubber, and filled in with silicone to achieve the necessary vacuum.

2.4. Medida de infrarrojos

The thermal images were acquired using the Optris PI 160 termographic camera (Optris GmbH, Berlin, Germany). It uses a two-dimensional focal plane array with 160x120 pixels, a spectral range of 7.5 to 13 μm, a resolution of 0.05 °C and an accuracy of $\pm$ 2 %. The camera

covers a temperature range of -20 to 900 °C. It has a field of vision of 23°x17° with a minimum distance of 2 cm. The camera uses Optris PI Connect software (Optris GmbH, Berlin, Germany).

3. Results and discussion

The temperature values obtained from the thermographic camera are not real, therefore, the correction developed by Traffano-Schiffo et al., 2014[7] was applied.

When the sublimation front advances, it alters the composition of the sample. The areas that have already been sublimated reduce their heat transmission because a loss of water, which causes a change in trend in the evolution of temperature with respect to time. Figure 1 shows this change in trend. So, the sublimation temperature and the process time can be extracted for each point of the sample's profile.
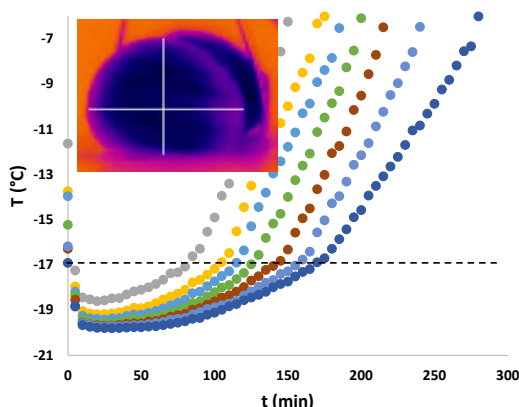
*Fig. 1 Evolution of the temperature for different points of the profile over time.*

With the sublimation temperature it is possible to calculate the water activity (a_w) using the Fontan and Chirife equation (1981) (Eq. 1).

$$-\ln(a_w) = 9.6934 \cdot 10^{-3} \cdot \Delta T_f + 4.761 \cdot 10^{-6} \cdot \Delta T_f^2 \qquad (1)$$

Where: ΔT_f = difference between the initial freezing temperature and the the sample (K).

From this a_w and the poultry sorption isotherm at low temperatures, it is possible to obtain the non-freezeable water fraction (x_w^{NF}) of the product at the sublimation time. The isotherm parameters modeled by GAB are $x_{w0} = 11.009 - 0.4589T + 0.0116T^2$; $C = -3423.2 + 1144T - 77.248T^2 + 1.4357T^3$; $K = 0.9419 - 0.0034T + 0.0006T^2 - 0.00001T^3$. Substracting to the overal water fraction, the non-freezeable water, it is possible to obtain the ice fraction.

Once the lyophilization process has begun, sample can be divided in two volumetric areas: the sublimated zone (partially dehydrated) and frozen zone, separated by the sublimation front (Fig. 2). When the frozen water sublimates, appears a vapour flux from the sublimation front to the surface, crossing the sublimated zone and evaporating a part of adsorved water by mechanical dragging. Mass of each zone throughout the process has been estimated using the volume difference between cylinders and the density of freeze-dried and frozen product.
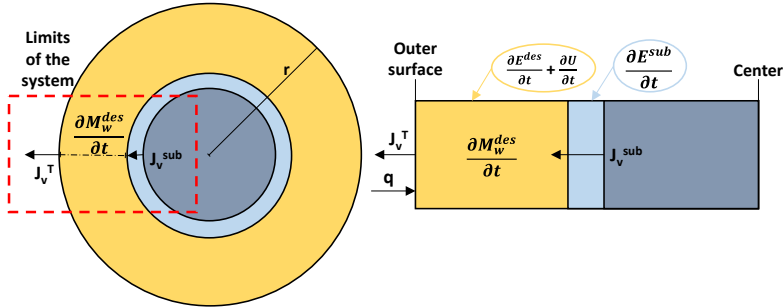
Fig. 2 Diagram of the different zones and phenomena. ☐ *Sublimated area;* ☐ *Sublimation front;* ☐ *Frozen zone. The limits of the system are highlighted in red, enlarged to the right with the molar and energy balances.*

In order to obtain the different mechanism involved in the freezedry process, it is necessary to estimate the water flux, using a molar water balance in the sublimated zone (Eq. 2).

$$J_v^T \cdot S_{ext} = J_v^{sub} \cdot S_{sub} + \frac{\partial M_w^{des}}{\partial t \cdot M_{rw}} \tag{2}$$

When the vapor flux comes from the sublimation can be calculated as follows (Eq. 3):

$$J_v^{sub} = \frac{x_w^f \cdot \rho_{wf} \cdot \Delta r}{\Delta t \cdot M_{rw}} \tag{3}$$

Where: J_v^T = overall vapour flux leaving the system (mol·s^{-1}·m^{-2}); S_{ext} = external surface of the cylinder (m^2); J_v^{sub} = sublimated vapour flux (mol·s^{-1}·m^{-2}); S_{sub} = surface of the sublimation front (m^2); M_w^{des} = evaporated water mass (kg); t = process time (s); x_{wf} = freezed water mass fraction (kg·kg^{-1}); ρ_{wf} = density of frozen water (kg·m^{-3}); M_{rw} = Molecular water mass (18 g·mol^{-1}). The last term of mass balance represents the negative accumulation of adsorved water molecules induced by mechanical drag of these molecules by the strong vapour streams produced in the sublimation front.

In order to continue determine the mechanism of water dehydration, the equation 4 that describes the free energy variation was applied[14].

$$dG = -SdT + VdP + Fdl + \psi de + \sum_i \mu_i \, dn_i \tag{4}$$

Where: SdT = entropic term related to heat flux; VdP = mechanical energies related to the variation of pressure; Fdl = mechanical energies related to the elongation force (resistance of the tissue to expand); ψde = effect of the electric field induced by ions; $\sum_i \mu_i \, dn_i$ = sumatory of the chemical potentials of the species "i", with the rest of the variables state are constant.

When the variation of free energy is represented per mole of water, the extended water chemical potential is obtained (Eq. 5).

$$\Delta\mu_w = \frac{\Delta G}{\Delta n_w} \tag{5}$$

Where: $\Delta\mu_w$ = water chemical potential (J·mol^{-1}); ΔG = Gibbs free energy variation (J); Δn_w = water moles (mol).

Combining the equations 4 and 5, the equation 6 is obtained, which describes the water chemical potential in the system described in figure 2 (sublimated zone) . In this equation, the last term is not included, because the desorption caused by the difference between water activities in the sample is negligible compared with the entropic term and those of mechanical energies. Moreover, ψde term also is negligible since the sample only presents native ions.

$$\Delta\mu_w^{des} = s_w\Delta T + v_w\Delta P + F_w dl \tag{6}$$

Where: s_w = partial water molar entropy (J·K^{-1}·mol^{-1}); ΔT = gradient of temperature between surface and sublimation front (K); v_w = partial water molar volume (m^3·mol^{-1}); ΔP = pressure variation (Pa); $F_w dl$ = elongation force (J). It is possible to estimate the entropic and the pressure term by using the sublimation temperature and its corresponded sublimation pressure obtained from Fig. 2.

Applying the Onsager relations[14], the water molar flux is related to the water chemical potential, working as a driving force for water transport, through the phenomenological coefficient (Eq. 7).

$$J_w^T = L_w \cdot \Delta\mu_w \tag{7}$$

Where: J_w = water molar flux (mol·s^{-1}·m^{-2}); L_w = phenomenological coefficient (mol^2·J^{-1}·s^{-1}·m^{-2}); $\Delta\mu_w$ = water chemical potential (J·mol^{-1}).

From the equation 7 it is possible to calculate the phenomenological coefficient after 200 min, where value remains constant because the sublimation front is reaching the center and the swelling resistance of the tissue is negligible (L_w = 1.14·10^{-5} mol^{2}J^{-1}s^{-1}m^{-2}). Therefore, applying this value along the treatment it is possible to estimate the elongation term (Fig 3a). Using the expansion of the sublimated area, and estimating the ice space loosed in the sublimation it is possible to calculate the increment of the porosity ($\Delta\varepsilon$). Fig. 3b shows the relation between the elongation term and the increment of the porosity, where it is possible to observe that the swelling process of tissue is proportional to the reduction of the elongation

term, reducing the swelling resistance of the tissue reaching its maximum expansion in its minimum resistance.
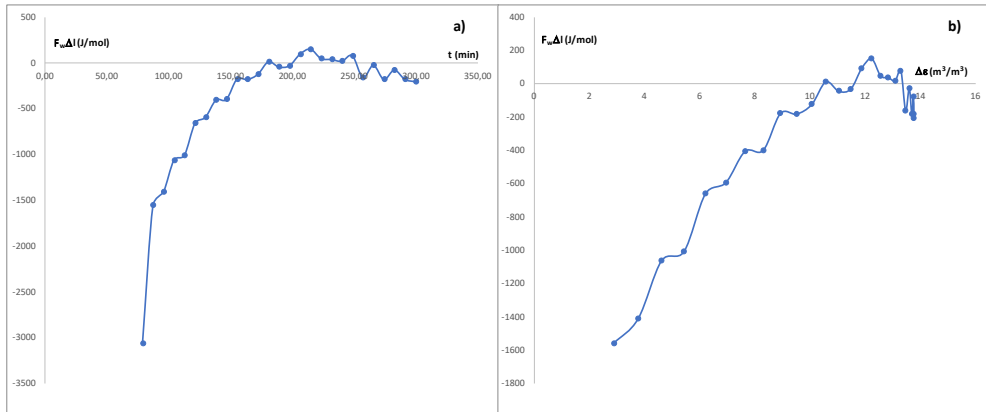

Fig. 3a Elongation term vs process time; 3b Elongation term vs increment of the porosity.

4. Conclusions

Has been developed a non-continuous irreversible thermodynamic model based in thermal infrared measures and in shrinkage/swelling mechanism that explains the behaviours produced throughout the meat freeze-drying process.

Acknowledgements

References

[1] Freire, F.B.; Vieira, G.N.; Freire, J.T.; Mujumdar, A.S. Trends in modeling and sensing approaches for drying control. Drying Technology 2014, 32(13), 1524–1532.

[2] Moses, J.A.; Norton, T.; Alagusundaram, K.; Tiwari, B.K. Novel drying techniques for the food industry. Food Engineering Reviews 2014, 6(3), 43–55.

[3] Ratti, C.; Hot air and freeze-drying of high-value foods: a review. Journal of Food Engineering 2001, 49, 311-319.

[4] Ramšak, M.; Ravnik, J.; Zadravec, M.; Hriberšek, M.; Iljaž, J. Freeze-drying modeling of vial using BEM. Engineering Analysis with Boundary Elements 2017, 77, 145-156.

[5] Duan, X.; Yang, X.; Ren, G.; Pang, Y.; Liu, L.; Liu, Y. Technical aspects in freeze-drying of foods. Drying Technology 2016, 34:11, 1271-1285.

[6] Talens, C.; Castro-Giraldez, M.; Fito, P.J. A thermodynamic model for hot air microwave drying of orange peel. Journal of Food Engineering 2016, 175, 33-42.

[7] Traffano-Schiffo, M.V.; Castro-Giraldez, M.; Fito P.J.; Balaguer, N. Thermodynamic model of meat drying by infrarred thermography. Journal of Food Engineering 2014, 128(0), 103-110.

[8] Clemente, G., Bon, J., Sanjuán, N., Mulet, A. Drying modelling of defrosted pork meat under forced convection conditions. Meat science 2011, 88(3), 374-378.

[9] Akanbi, C.T.; Adeyemi, R.S.; Ojo, A. Drying characteristics and sorption isotherm of tomato slices. Journal of food engineering 2006, 73(2), 157-163.

[10] Hammami, C.; Rene, F. Determination of freeze-drying process variables for Strawberries. Journal of Food Engineering 1997, 32, 133-154.

[11] Irzyniec, Z.; Klimczak, J.; Michalowski, S. Freeze-Drying of the black currant juice. Drying Technology 2007, 13:1-2, 417-424

[12] Nakagawa, K.; Ochiai, T. A mathematical model of multi-dimensional freeze-drying for food products. Journal of Food Engineering 2015, 161, 55-67.

[13] Vadivambal, R.; Jayas, D.S. Applications of thermal imaging in agriculture and food industry-a review. Food and Bioprocess Technology 2011, 4(2), 186-199.

[14] Castro-Giraldez, M.; Fito, P.J.; Fito P. Non-equilibrium thermodynamic approach to analyze the pork meat (Longissimus dorsi) salting process. Journal of Food Engineering 2010, 99(1), 24-30.